Am J Physiol Renal Physiol. Author manuscript; available in PMC 2016 July 25.

Published in final edited form as:

Am J Physiol Renal Physiol. 2015 August 15; 309(4): F383–F392. doi:10.1152/ajprenal.00464.2014.

Carbonic anhydrase II binds to and increases the activity of the epithelial sodium-proton exchanger, NHE3

Devishree Krishnan[1,3], **Lei Liu**[1], **Shane A. Wiebe**[1,3], **Joseph R. Casey**[1,2,3], **Emmanuelle Cordat**[1,3], and **R. Todd Alexander**[1,3,4]

[1]Department of Physiology, University of Alberta, Edmonton, Alberta, Canada

[2]Department of Biochemistry, University of Alberta, Edmonton, Alberta, Canada

[3]Membrane Protein Disease Research Group, University of Alberta, Edmonton, Alberta, Canada

[4]Department of Pediatrics, University of Alberta, Edmonton, Alberta, Canada

Abstract

Two-thirds of sodium filtered by the renal glomerulus is reabsorbed from the proximal tubule via a sodium/proton exchanger isoform 3 (NHE3)-dependent mechanism. Since sodium and bicarbonate reabsorption are coupled, we postulated that the molecules involved in their reabsorption [NHE3 and carbonic anhydrase II (CAII)] might physically and functionally interact. Consistent with this, CAII and NHE3 were closely associated in a renal proximal tubular cell culture model as revealed by a proximity ligation assay. Direct physical interaction was confirmed in solid-phase binding assays with immobilized CAII and C-terminal NHE3 glutathione-*S*-transferase fusion constructs. To assess the effect of CAII on NHE3 function, we expressed NHE3 in a proximal tubule cell line and measured NHE3 activity as the rate of intracellular pH recovery, following an acid load. NHE3-expressing cells had a significantly greater rate of intracellular pH recovery than controls. Inhibition of endogenous CAII activity with acetazolamide significantly decreased NHE3 activity, indicating that CAII activates NHE3. To ascertain whether CAII binding per se activates NHE3, we expressed NHE3 with wild-type CAII, a catalytically inactive CAII mutant (CAII-V143Y), or a mutant unable to bind other transporters (CAII-HEX). NHE3 activity increased upon wild-type CAII coexpression, but not in the presence of the CAII V143Y or HEX mutant. Together these studies support an association between CAII and NHE3 that alters the transporter's activity.

Keywords

NHE3; carbonic anhydrase II; sodium; pH

Address for reprint requests and other correspondence: R. T. Alexander, Dept. of Pediatrics, 4-585 Edmonton Clinic Health Academy, 11405 87th Ave., Univ. of Alberta, Edmonton, Alberta, T6G 2R7, Canada, todd2@ualberta.ca.

DISCLOSURES

No conflicts of interest, financial or otherwise, are declared by the authors.

AUTHOR CONTRIBUTIONS

Author contributions: D.K., S.A.W., J.R.C., E.C., and R.T.A. provided conception and design of research; D.K., L.L., S.A.W., and R.T.A. performed experiments; D.K., L.L., S.A.W., and R.T.A. analyzed data; D.K., L.L., S.A.W., J.R.C., E.C., and R.T.A. interpreted results of experiments; D.K. and R.T.A. prepared figures; D.K. and R.T.A. drafted manuscript; D.K., L.L., S.A.W., J.R.C., E.C., and R.T.A. approved final version of manuscript; J.R.C., E.C., and R.T.A. edited and revised manuscript.

Intravascular volume is maintained via highly regulated control of sodium homeostasis, best observed along the course of the nephron, where the majority (at least 65%) of Na^+ is reabsorbed from the proximal tubule. Transepithelial reabsorption of sodium from this nephron segment is determined by a series of transport events and enzyme-mediated catalysis. Apical Na^+ influx occurs through the sodium/proton exchanger isoform 3 (NHE3) in exchange for a cytosolic H^+. Cytosolic Na^+ is excreted back into the blood via either the Na^+-K^+-ATPase or the sodium-dependent bicarbonate transporter (NBCe1). The rate-limiting step is apical Na^+ influx via NHE3, whose activity depends on the presence of cytosolic protons. H^+ is generated by the cytosolic carbonic anhydrase isoform II (CAII), an enzyme mediating the catalysis of CO_2 and H_2O into HCO_3^- and a H^+. H_2O and CO_2 enter the cell from the tubular lumen, at least in part through the water channel aquaporin-1 (11, 23, 27). This process also drives HCO_3^- reabsorption, as glycosylphosphatidylinositol (GPI)-linked extracellular carbonic anhydrase IV mediates catalysis of effluxed H^+ to convert HCO_3^- into H_2O and CO_2 (40).

NHE3 is one of nine isoforms of the Na^+/H^+ exchanger family (14). In mammals, NHE1-5 proteins are present in the plasma membrane, and NHE6-9 localize predominantly in endomembrane compartments (13, 14). NHE3 is located in the apical membrane of intestinal and renal epithelia (19). In the kidney, NHE3 is predominantly expressed in the proximal tubule and to a lesser extent in the thick ascending limb of the loop of Henle (9). NHE3 participates directly in Na^+ reabsorption and indirectly in the reabsorption of bicarbonate, Ca^{2+}, and the secretion of ammonium (10, 20, 25).

CAII both physically and functionally interacts with a number of transporters, including anion exchanger 1 (AE1), NBCe1, and MCT (6, 7, 24, 38, 39). The best characterized interaction is between AE1 and CAII. An LDADD motif in the cytosolic C terminus of AE1 binds to the histidine-rich N terminus of CAII (37, 39). This interaction augments AE1 transport, potentially via enzymatic provision of substrate to the transporter (38). Such an interaction has been dubbed a transport metabolon (33). NHE1 directly interacts with the cytosolic carbonic anhydrase CAII, through the NHE1 ^{790}RIQRCLSDPGPHP^{802} motif in the carboxyl, cytosolic terminus (16, 17). This interaction increases NHE1 activity (16). However, the existence of a direct AE1/CAII physical interaction has been questioned (1, 22).

Examination of the cytosolic C terminus of NHE3 revealed a potential CAII binding site (^{710}IKEKDLELSDTEE^{722}), consistent with the motif established for NHE1 (16, 17). Given this, and the known dependence of CAII activity for what is currently appreciated as NHE3-mediated transepithelial Na^+ transport (12, 26), we hypothesized that CAII and NHE3 physically and functionally interact. Consistent with this, a proximity ligation assay (PLA) revealed the close association of the two proteins; we could coimmunoprecipitate CAII with NHE3, and a microtiter plate assay confirmed that the glutathione-*S*-transferase (GST)-tagged NHE3 C-terminal domain, containing the putative CAII binding site, binds CAII. Moreover, in the presence of CO_2 and bicarbonate, NHE3 activity is inhibited by acetazolamide, but is not when NHE3 activity is measured in the nominal absence of CO_2 and HCO_3^-.

MATERIALS AND METHODS

Materials

Restriction enzymes *Eco*R1 and *Not*I were from New England Biolabs (Whitby, ON). BL21 *Escherichia coli* and pcDNA 3.1+ were from Invitrogen (Carlsbad, CA). pGEX 6P-1 and glutathione-Sepharose 4B were from GE Healthcare (Mississauga, ON). Recombinant human CAII, nigericin, acetazolamide, and EIPA were from Sigma-Aldrich Canada (Oakville, ON). Antibodies/stains used include rabbit anti-CAII polyclonal antibody (Santa Cruz Biotechnology, Santa Cruz, CA), mouse anti-hemagglutinin (HA; 16B12, Covance, Emeryville, CA), and phalloidin (Invitrogen). DMEM-F12 medium, geneticin, penicillin/streptomycin/glutamine (PSG), and neon transfection reagents were from GIBCO Life Technologies (Burlington, ON). Fetal bovine serum was from VWR International (Mississauga, ON). Opossum kidney cells were from the American Type Culture Collection (ATCC; Manassas, VA). Fugene was from Promega (Madison, WI). Isopropyl β-D-1-thiogalactopyranoside (IPTG) was from Fermentas Canada, (Burlington, ON).

Cell culture

Opossum kidney (OK) cells were obtained from ATCC. OK cells stably overexpressing NHE3 with three exofacial HA tags, $NHE3_{38HA3}$ (amino acid sequence: YPYDVPDYAS) (2), or pcDNA 3.1+ were generated by transfecting the constructs with FuGENE 6 transfection reagent, then selecting with geneticin. Monoclonal stable cell lines were subsequently isolated by limiting dilution as previously (20). The cells were maintained in DMEM-F12 medium supplemented with 10% fetal bovine serum, 5% penicillin, streptomycin glutamine (PSG), and 750 μM geneticin (G418) at 37°C in a 5% CO_2 incubator.

OK cells stably expressing $NHE3_{38HA3}$ were transiently transfected with cDNA encoding CAII, CAII-myc, an inactive mutant of CAII (CAII-V143Y) (33), a binding mutant of CAII [CAII-HEX, which is a catalytically active mutant, containing six point mutations (H3P, H4D, K9D, H10K, H15Q, and H17S)] (37), or pcDNA 3.1+, via electroporation with the Neon transfection system (4). For experimental purposes, transfected cells were grown on 11 × 7.5-mm-2D-UAB (Thermo Scientific, Asheville, NC) coverslips.

Immunoblotting

Stably or transiently transfected cells were grown on 10-cm-diameter tissue culture dishes. Cell lysates were prepared with sample buffer containing 4.6% SDS, 0.02% bromophenol blue, 20% glycerol, 2% 2-mercaptoethanol, 130 mM Tris·HCl, pH 6.8, with protease inhibitor cocktail (Calbiochem, Gibbstown, NJ), and benzonase nuclease (Novagen, EMD Chemicals, San Diego, CA). Total cell lysate was incubated at 37°C for 20 min and then was fractionated on a 12% polyacrylamide gel and then transferred to a polyvinylidene difluoride membrane. The membrane was first blocked with 5% milk in TBST (150 mM NaCl, 0.1% Tween, 20 mM Tris, pH 7.4) for 2 h at room temperature. Then it was immunoprobed with mouse monoclonal anti-HA antibody (16B12, Covance, Emeryville, CA), rabbit anti-CAII (Santa Cruz Biotechnology), or mouse monoclonal anti-Myc antibody (Cell Signaling Technology, Danvers, MA), all in 1:1,000 dilution, incubated overnight at 4°C. Membranes

were washed with TBST then incubated with either secondary horseradish peroxidase (HRP)-conjugated goat anti-mouse or goat anti-rabbit IgG antibody (1:5,000 dilution in TBST, Santa Cruz Biotechnology) for 2 h at room temperature. Finally, the membranes were washed with TBST and after incubation with western Lighting plus ECL reagents (PerkinElmer, Boston, MA), immunoreactive bands were visualized with a Carestream Advanced Fluorescent Imaging F PRO image station (Carestream Health, Rochester, NY).

Measurement of Na^+/H^+ exchange activity in the presence of CO_2

To assess a functional interaction between NHE3 and CAII, we overexpressed NHE3 containing three exofacial HA tags in OK cells to enhance NHE3 expression (20). NHE activity was measured in cells that were grown on coverslips (11 × 7.5 mm, Thermo Scientific) as previously (16). Coverslips were incubated with 5 mM BCECF-AM (Molecular Probes, Eugene, OR) at 37°C for 10 min. The loaded cells were rinsed with iso Na^+ buffer (140 mM NaCl, 1 mM $MgCl_2$, 1 mM $CaCl_2$, 3 mM KCl, 10 mM glucose, and 5 mM HEPES, pH 7.4) to remove excess probe and then placed inside a fluorescence cuvette where the coverslip was held immobile with a holder device. Intracellular pH (pH_i) was determined with a PTI-Fluorometer [LPS-220B, Photon Technology International (PTI), London, ON]. The NHE activity of OK cells overexpressing NHE3 or pcDNA3.1+ was measured as the rate of pH recovery after acidifying cells by switching them from iso Na^+-buffered medium to a HCO_3^--buffered medium (130 mM NaCl, 1 mM $MgCl_2$, 1 mM $CaCl_2$, 3 mM KCl, 10 mM glucose, and 25 mM $NaHCO_3$, pH 7.4), bubbled with 5% CO_2-95% air; the perfusion rate was kept constant per experimental condition but varied between sets of experiments from 1.5–8 ml/min to ensure equivalent degree of acidification within experimental groups. Fluorescence measurements were made with dual excitation (440, 490 nm), and a single emission was measured (510 nm). Calibration was performed with high K^+-containing buffer at pH 6.0, 6.5, 7.0, and 7.5 (140 mM KCl, 1 mM $MgCl_2$, 1 mM $CaCl_2$, 10 mM glucose, and 20 mM HEPES) containing 10 mM nigericin for each individual coverslip (34). NHE3 activity was then calculated as the rate of change in pH over the first 30 s from maximal acidification. The rate of pH change was also assessed in the presence of 100 μM EIPA and acetazolamide (Sigma-Aldrich Canada) when indicated.

Measurement of Na^+/H^+ exchanger activity in the absence of CO_2

NHE3 activity was assessed in the absence of CO_2 as previously (2, 3). After loading with BCECF-AM as above, the cells were rinsed with iso Na^+ buffer (140 mM NaCl, 1 mM $MgCl_2$, 1 mM $CaCl_2$, 3 mM KCl, 10 mM glucose, and 5 mM HEPES, pH 7.4) to remove excess probe and then placed inside a fluorescence cuvette where the coverslip was held immobile with a holder device. pH_i was determined with a PTI-Fluorometer (LPS-220B, PTI). The cells were perfused with iso Na^+ buffer, containing 10 mM NH_4Cl for 10 min before a switch to acidify the cells by perfusing with iso K^+ buffer (140 mM KCl, 1 mM $MgCl_2$, 1 mM $CaCl_2$, 10 mM glucose, and 20 mM HEPES, pH 7.4) for 2 min. pH recovery in cells transfected with NHE3 or pcDNA3.1+ was then induced by perfusing cells with iso Na^+ buffer. Calibration was performed with high K^+-containing buffer with 10 mM nigericin for each individual coverslip as above (34). NHE3 activity was calculated as the change in pH over the first 30 s after iso Na^+ readdition.

Generation of glutathione-S-transferase constructs and CAII-myc

DNA encoding amino acids 630–730 or 730–830 of rat NHE3 was amplified by PCR. The former region contains a homologous region to the NHE1, CAII binding site (^{710}IKEKDLELSDTEE^{722}) (17). Rat full-length NHE3 was used as the template (2). Primers for the 630–730 region were forward: 5′-CG GAA TTC CTC TAC AGT CGG CAC GAG CT-3′ and reverse: 5′-G GGC GGC CGC TCA ATG CCT CCA CTG ATC TCT TC-3′. Primers for the 730–830 region were forward: 5′-CG GAA TTC GAA TTT CTG GCC AGC GTC AC-3′ and reverse: 5′-G GGC GGC CGC TCA CAT GTG TGT GGA CTC AGG G-3′. Forward primers contained an *Eco*RI restriction site and reverse primers a *Not*I site. After amplification, the PCR fragment was digested with the appropriate enzymes and then ligated into the pGEX 6P1 vector. The generated constructs are subsequently referred to as NHE3-Tail-1 (630–730) and NHE3-Tail-2 (730–830).

CAII-myc was subcloned from a CAII-GFP construct by PCR with forward primer 5′-CCG GAA TTC CGG GCC ACC ATG TCC CAT CAC TGG GGG TAC G-3′ and reverse primer 5′-AAGGAAAAAA GC GGC CGC TTA TAG GTC CTC CTC GGA GAT CAG CTT TTG TTC TTT GAA GGA AGC TTT GAT TTG CCT G-3′. *Eco*RI and *Not*I restriction sites were engineered into the primers, permitting digestion and ligation into the pcDNA 3.1+ mammalian expression vector. The construct was found to be functional by measuring the rate that lysate from cells overexpressing it acidified a solution bubbled with CO_2 (5). All DNA sequences were confirmed by sequencing at the TAGC Applied Genomics core, University of Alberta.

Purification of glutathione-S-transferase fusion proteins

GST. NHE3-Tail-1, GST.NHE3-Tail 2, or pGEX 6P1 (empty vector) were purified by methods used previously (16, 32). They were transformed into *E. coli* BL21 by electroporation (Eppendorf Electroporator 2510, Eppendorf North America, Westbury, NY) and then plated onto LB agar plates with 100 μg/ml ampicillin (Sigma-Aldrich Canada) and incubated at 37°C overnight. A single colony was used to inoculate LB broth, containing 100 μg/ml of ampicillin, which was then incubated overnight at 37°C in a shaker (Infors HT Ectron, Infors Canada, Anjou, Quebec). A 5-ml culture was subsequently inoculated into 250 ml of LB broth and grown at 37°C in a shaker until it reached A_{600} 0.6–1.0. Isopropylthiogalactoside (1 mM final concentration) (Fermentas/Thermo Scientific, Ottawa, ON) was added, and the culture was subsequently incubated for 3 h further at 37°C while shaking. Cultures were then centrifuged at 7,500 *g* for 10 min in a Beckman-Avanti J-25 centrifuge (Beckmann Coulter, Mississauga, ON) at 4°C. The bacterial pellet was resuspended in 5 ml of 4°C PBS with benzamidine, PMSF, and protease inhibitor cocktail (Roche Diagnostics, Laval, Canada) with 75 μl of Triton X-100. Suspended cells were disrupted by sonicating (Braunsonic 2000 sonicator) with four 45-s pulses at 20 kHz. Cells were then centrifuged at 12,000 *g* for 10 min at 4°C. The supernatant was transferred to glutathione Sepharose 4B resin (washed with PBS) and incubated at 20°C for 2 h. The samples were subsequently centrifuged at 1,500 *g* for 5 min and then washed with PBS. The fusion proteins were eluted with glutathione buffer (10 mM reduced glutathione in 50 mM Tris·HCl, pH 8.0). The concentration of protein was determined by measuring A_{280} with a

Nanodrop spectrophotometer, an extinction coefficient of 1 mg/ml (NanoDrop 2000c UV-Vis Spectrophotometers, Thermo Scientific) and BSA standards.

Microtiter plate binding assay

A microtiter plate binding assay was used to assess a physical interaction between NHE3 and CAII, as per other transporter-CAII interactions (16, 38). Human recombinant CAII (25 nM) was coated on 96-well microtiter plates (96-well EIA/RIA plate, Costar 3590, Corning, Corning, NY) for 30 min at room temperature in ELISA buffer (150 mM NaCl, and 100 mM Na_2HPO_4, pH 6.0) with 1.25 mg/ml of *N*-cyclohexyl-*N*-carbodiimide metho-*p*-toluene sulfonate (Sigma-Aldrich Canada). Plates were washed with PBS before blocking with 2% bovine serum albumin in PBS for 2 h at 20°C. Plates were then washed with PBS and subsequently overlaid with either NHE3-Tail-1, NHE3-Tail-2, or GST alone (50–400 nM) in antibody buffer (100 mM NaCl, 5 mM EDTA, 0.25% gelatin, 0.05% Triton X-100, and 50 mM Tris, pH 7.5), containing 1 mM DTT at 20°C for 16 h. Note that for experiments examining the effect of pH, the amount of NaCl or pH of solution was altered to the stated content. Plates were next washed with PBS, and the samples were incubated with a rabbit polyclonal anti-GST antibody (1:5,000, Santa Cruz Biotechnolgy) for 2 h at 20°C. After washing with PBS, plates were incubated with a donkey anti-rabbit IgG polyclonal antibody (1:5,000, Santa Cruz Biotechnolgy), washed again with PBS, and finally incubated with streptavidin conjugated to HRP (Pierce Biotechnology, Rockford, IL) for 1 h at 20°C. Plates were developed with TMB substrate reagent (San Jose, CA) and then stopped by adding 200 μl/well of 5 M H_2SO_4. The relative amount of GST-fusion protein binding was finally measured at A_{450} nm in a Synergy Biotek microplate reader.

PLA

An association between NHE3 and CAII was assessed by PLA using a previously established methodology (30, 36). OK cells were transfected with cDNA encoding either NHE3 (2), human AE1 (37, 39), or human concentrative nucleoside transporter (hCNT3) (41) and myc-tagged CAII. Two days after transfection, the cells were washed with PBS, lysed in IPB buffer (1% NP-40, 5 mM EDTA, 0.15 M NaCl, 0.5% deoxycholate, and 10 mM Tris·HCl, pH 7.5) containing protease inhibitors, washed twice in PBS, and then fixed (3.5% paraformaldehyde, 1 mM $CaCl_2$, 1 mM $MgCl_2$ in PBS, pH 7.4 for 20 min). They were then washed twice with PBS and finally quenched with 50 mM NH_4Cl for 10 min. Fixed cells were permeabilized with 0.1% Triton X-100 in PBS for 1 min at 20°C and then washed twice for 5 min with Wash Buffer A (Olink Bioscience, Uppsala, Sweden). Samples were then processed for PLA using the Duolink Detection kit (Olink Bioscience), according to the manufacturer's instructions. Briefly, the cells were blocked with manufacturer-provided blocking solution for 30 min at 37°C, incubated for 1 h at 37°C in a humidified chamber with a 1:1,000 dilution of rabbit anti-CAII antibody and either mouse anti-HA, IVF12 mouse monoclonal anti-AE1 (a gift from Dr. Michael Jennings, Univ. of Arkansas, Little Rock, AR), or mouse monoclonal anti-hCNT3 (a gift from Dr. James Young, Univ. of Alberta, Edmonton, AB) (41) at 1:500, 1:1,000, and 1:500 dilutions in antibody diluent, respectively. Samples were then washed twice for 5 min in wash *buffer A* (manufacturer provided), and then incubated for 1 h at 37°C with a combination of the corresponding PLA probes (anti-rabbit Plus and anti-mouse Minus, both supplied by the manufacturer)

conjugated to specific oligonucleotides. The PLA oligonucleotides were hybridized and circularized by ligation (30 min at 37°C), and the DNA circle formed was amplified by rolling circle amplification into single-stranded DNA anchored to one of the antibodies. The amplification product was detected by addition of complementary oligonucleotides labeled with Texas Red fluorophore. Coverslips were mounted in the provided mounting medium and observed through a 60X/1.42 PlanApo oil-immersion objective of a spinning-disk confocal microscope (WaveFx, Quorum Technologies, Guelph, ON) on an Olympus IX-81 inverted stand (Olympus, Markham, ON). *Z*-stack confocal image capture was performed with a C9100-13 EM-CCD Digital Camera (Hamamatsu, Hamamatsu City, Japan), using Volocity software (PerkinElmer, Mississauga ON).

Coimmunoprecipitation

Coimmunoprecipitation (IP) was performed essentially as previously (4). OK cells were cotransfected with $NHE3_{38HA3}$ and CAII-myc by neon transfection as per the PLA (see above). The cells were grown in 10-cm tissue culture dishes for 2 days in DMEM-F12 media in the presence of 5% CO_2 at 37°C. Once they were 100% confluent, the cells were washed with PBS then collected with 200 μl of elution buffer (1% NP-40, 5 mM EDTA, 0.15 M NaCl, and 10 mM Tris·HCl, pH 8.1) containing protease inhibitor cocktail (1:100, Calbiochem) and PMSF (1:1,000). The homogenized cell lysate was placed on ice for 30 min, then centrifuged at 12,000 rpm for 10 min at 4°C. The supernatant was subsequently collected, and the concentration of protein was determined by measuring A_{280} with a Nanodrop spectrophotometer (NanoDrop 2000c UV-Vis Spectrophotometers, Thermo Scientific), using an extinction coefficient of 1 mg/ml and BSA standards. Two separate 50-μl aliquots of Dynabeads protein G (Thermo Fischer) were precleared and then rinsed with 100 μl of elution buffer. To one sample of beads, 2 μg of goat anti-HA antibody was added; to the other sample, 2 μg of rabbit serum was added. Both were then incubated on ice for 20–30 min. Protein cell lysate (300 μg) was added with elution buffer to make the total volume 250 μl, and the samples were incubated overnight at 4°C. The next day the beads, were washed three times with elution buffer containing protease inhibitor cocktail and PMSF. Finally, to elute the bound protein from the beads, 40 μl of sample buffer was added to either the CO-IP, or control sample and to a total protein lysate sample (50 μg), and incubated at 37°C for 20 min. The samples were then subjected to SDS-PAGE and immunoblotting with anti-myc as above.

Statistical analysis

Data are presented as means ± SE. Paired or unpaired Student's *t*-tests or ANOVA was carried out to determine statistical significance as appropriate. Tests were performed using Excel software (Microsoft, Santa Monica, CA), and P values < 0.05 were considered statistically significant.

RESULTS

Acetazolamide inhibits NHE3 activity in the presence of CO_2 and HCO_3^-

To assess whether a functional interaction between NHE3 and CAII exists, we stably expressed NHE3 with three exofacial HA epitopes in OK cells (OK-$NHE3_{38HA3}$) (2). This

both increased NHE3 expression and activity in this cell line but also provided an epitope tag greatly facilitating NHE3 detection and manipulation (3, 20). Cell lysate immunoblotted for the HA epitope revealed a single band of the appropriate molecular weight in cells expressing $NHE3_{38HA3}$, but not cells expressing the vector alone (Fig. 1*A*). Immunoblotting of the same cell lysate revealed endogenous expression of CAII (Fig. 1*B*, *bottom* band). Immunostaining of OK cells with HA antibody and 4,6-diamidino-2-phenylindole to stain nuclei found NHE3 predominantly present in the apical membrane of OK cells (Fig. 1*C*), consistent with its localization in vivo.

NHE3 activity was then assessed as the rate of recovery of pH_i induced by an acid load and measured with the fluorescent radiometric pH sensitive dye BCECF-AM. The cells were acidified by switching them from a bicarbonate-free medium to one containing bicarbonate and bubbled with 5% CO_2. OK-$NHE3_{38HA3}$ cells demonstrate significantly greater Na^+-dependent recovery of pH_i than vector-transfected controls (Fig. 1, *D*–*G*). Recovery from an acid load under these conditions was both Na^+ dependent (Fig. 1, *D* and *E*) and inhibited by 100 μM EIPA (Fig. 1, *F* and *G*), a dose sufficient to block NHE3 activity (35). Recovery from a CO_2-induced acid load was also prevented when a choline-HCO_3-containing buffer was used instead of the $NaHCO_3$ ($dpH_i/dT = 0.0014 \pm 0.0005$ in the presence of Na^+ vs. -0.0004 ± 0.0002 in the absence). This is consistent with NHE3 activity and not the activity of either a bicarbonate transporter or an H^+-ATPase. To examine the possibility of a functional interaction between NHE3 and CAII, we inhibited endogenous CAII with acetazolamide and then repeated the measurement. This greatly attenuated NHE3 activity in the overexpressing cells (Fig. 2), consistent with a requirement for CAII activity to significantly augment NHE3 activity.

Acetazolamide does not inhibit NHE3 activity in the absence of CO_2

To ascertain whether the effect of acetazolamide on NHE3 activity was via inhibition of CAII per se and not by blocking NHE3 directly, we repeated the assay in the absence of bicarbonate and CO_2, in cells acidified by an ammonium chloride prepulse. Under these conditions, cells stably expressing NHE3 also demonstrated significant recovery from an acid load, which was Na^+ dependent and inhibited by 100 μM EIPA (Fig. 3, *A* and *B*). However, under these conditions, acetazolamide had no effect on the rate of recovery from an acid load in NHE3-expressing cells (Fig. 3, *C* and *D*). These results are consistent with CAII increasing NHE3 activity and not with acetazolamide directly inhibiting NHE3.

CAII association and activity are necessary to enhance NHE3 activity

To confirm that CAII activity is required to augment NHE3-mediated transport, we overexpressed $NHE3_{38HA3}$ with either wild-type CAII or the catalytically inactive CAII mutant (CAII-V143Y) (33) and then repeated the functional assay in the presence of bicarbonate and CO_2. The rate of pH_i recovery was significantly higher in cells expressing NHE3 than in those expressing CAII alone (Fig. 4, *A* and *B*). NHE3 activity was further increased by coexpression with wild-type CAII. However, this increase in activity was not observed when the catalytically inactive CAII-V143Y was coexpressed with NHE3 (Fig. 4, *A* and *B*). These studies revealed an increase of NHE3 activity induced by CAII but not catalytically inactive CAII (Fig. 4, *A* and *B*).

To assess whether CAII activity was sufficient to enhance NHE3 activity, we overexpressed NHE3 with a CAII mutant that fails to bind other transporters due to elimination of an N-terminal polybasic sequence, CAII-HEX (7, 37), and repeated the functional studies in the presence of bicarbonate and CO_2. Coexpression with CAII-HEX did not increase NHE3 activity beyond coexpression with the empty vector alone (Fig. 4, *A* and *B*). Importantly, when we immunoblotted the remaining cells for NHE3 or CAII we did not observe a significant difference in expression of either protein (Fig. 4, *C* and *D*). Taken together, these results demonstrate that CAII activity and physical interaction are required to increase NHE3 activity.

NHE3 and CAII associate closely

NHE3 and CAII are both expressed in the brush-border membrane of the proximal tubule (9, 36); however, given the resolution of the light microscope, these two proteins could still be 250 nm away from one another. To assess a closer physical interaction, we cotransfected myc-tagged CAII and either NHE3, hCNT3, or AE1 and then performed a PLA (30). hCNT3 is a plasma membrane nucleoside transport protein, not known to interact with CAII, while a CAII-AE1 coassociation has been reported previously, including by PLA (36, 38). We observed a PLA signal when AE1 and CAII were coexpressed, indicating the ability of the PLA to detect a protein-protein interaction. The absence of a PLA signal in CAII- and hCNT3-coexpressing cells illustrates the specificity of the PLA technique (Fig. 5, *A* and *B*). The coexpression of NHE3 and CAII also generated a significant PLA signal consistent with a close association of the two proteins (Fig. 5*C*). Importantly, we were able to detect all transfected proteins on immunoblots, indicating that the lack of a PLA signal in CAII- and hCNT3-coexpressing cells did not arise from the absence of protein expression (Fig. 5*D*).

CAII binds the C terminus of NHE3

To determine whether NHE3 and CAII physically associate, we coexpressed $NHE3_{38HA3}$ and CAII-myc in OK cells. We then immunoprecipitated NHE3 with an anti-HA antibody and immunoblotted with anti-myc. We used total protein cell lysate as a positive control and immunoprecipitated with rabbit serum as a negative control. CAII was immunoprecipitated by NHE3, but not rabbit serum (Fig. 6*A*). To examine whether there is a direct physical interaction between the cytosolic carboxyl terminus of NHE3 and CAII, we expressed amino acids 630–730 (NHE3-Tail-1) or 730–831 (NHE3-Tail-2) of rat NHE3 as GST fusion proteins (Fig. 6*B*). NHE3-Tail-1 contains the putative CAII binding site (^{710}IKEKDLELSDTEE^{722}). We then performed a microtiter plate binding assay with these two constructs (16). Recombinant human CAII was fixed to the plate and then overlaid with different concentrations of the GST-fusion protein (50–400 nM). The degree of binding was then assessed by applying an anti-GST antibody followed by a HRP secondary and measuring the development of a colorimetric reaction. The assay was also performed with GST alone, and the results were subtracted from both Tail constructs. We observed significantly greater binding of NHE3-Tail-1 to CAII than NHE3-Tail-2 (Fig. 6*C*). These data infer a direct interaction between the cytosolic terminus of NHE3 and CAII.

Finally, we tested the effects of varying pH and ionic strength on the interaction between CAII and NHE3, using the microtiter plate assay. Binding of GST alone was measured and

subtracted from all values. Maximal binding between NHE3-Tail-1 and CAII occurred at 100 mM NaCl; this was set to 100% (Fig. 7*A*). Increasing ionic strength past this decreased the interaction, and above 400 mM NaCl completely eliminated the interaction (Fig. 7*A*). We found that the NHE3/CAII interaction was strongly pH dependent. There was increased interaction at an alkaline pH (>8.0), and the interaction was prevented at an acidic pH, i.e., <6.0 (Fig. 7*B*). Half-maximal binding was observed at pH ~7.2. Therefore, the interaction between NHE3 and CAII is dependent on both ionic strength and pH, consistent with an electrostatic interaction.

DISCUSSION

NHE3 has an important role in renal function by reabsorbing Na^+, HCO_3^-, and H_2O from the proximal tubule (28). We provide several lines of evidence that NHE3 and CAII physically interact. A PLA confirmed a close association of the two proteins when expressed in a proximal tubular epithelial cell culture model. CO-IP confirmed a physical association between NHE3 and CAII and microtiter plate assays identified a region in the cytosolic terminus of NHE3 required for CAII binding. We also provide evidence that NHE3 and CAII functionally interact. Coexpression of NHE3 with CAII increased NHE3 activity, which depended on CAII catalysis, since augmented NHE3 activity was only prevented by acetazolamide in the presence of CAII substrate. Moreover, coexpression of NHE3 and a catalytically dead CAII did not increase NHE3 activity. Finally, a NHE3-CAII physical interaction is required to increase NHE3 activity, as a CAII construct lacking the putative transporter-binding motif failed to increase NHE3 activity. Together, these data support a physical and functional interaction between CAII and NHE3 in the proximal tubule.

We examined the interaction between NHE3 and CAII in a proximal tubule model, as this is a site of prodigious sodium and water reabsorption facilitated in large part by NHE3 activity (28). NHE3-CAII cooperation likely helps to maximize NHE3 function, permitting this process. NHE3 is also expressed throughout the intestine, where it plays a similar role in sodium and water reabsorption (15, 28). CAII is also expressed throughout the small and large bowel (18, 21, 29). We thus speculate that a physical and functional interaction between NHE3 and CAII in the mucosal membrane of the intestine may also serve to increase sodium and water absorption there.

CAII forms a transport metabolon with AE1, enhancing its activity (33). A metabolon is a complex of enzymes from one metabolic pathway coupled together so as to facilitate substrate movement from one active site to the next (31). Transport metabolons are a functional coupling of an enzyme to a transporter that increases flux through the transporter. The AE1 transport metabolon appears to require a direct physical interaction between the enzyme and the transporter (33), although there are also data suggesting a direct physical interaction is not required (1, 22). NHE1 and CAII also physically and functionally interact (16). Using similar experimental approaches, we found that both the putative transporter binding site in CAII and CAII catalysis are necessary to increase NHE3 activity. The interaction between NHE3 and CAII is different from the interaction between CAII and the monocarboxylate transporters, as CAII activity is required for increased NHE3 activity (7,

8). Our observations therefore support a mechanism whereby association of CAII with NHE3 increases transporter activity.

We found that the region between amino acids 630 and 730 in the cytosolic carboxy terminus of NHE3 binds CAII. We found this interaction to be pH sensitive. Consistent with a role for amino-terminal CAII histidine residues in mediating the interaction with NHE3, the interaction was titrated with a pK_a of 7.2, and enhanced at alkaline pH. This pK_a is nearly identical to the pK_a established for the AE1-CAII interaction, which is mediated through amino-terminal histidines in CAII, as mutation of histidine residues in the CAII N-terminal region prevents binding to AE1 (37, 38). Increasing ionic strength inhibited the NHE3-CAII interaction, suggesting that it is potentially an ionic interaction. Although the interaction was also inhibited at lower ionic strength, perhaps due to another factor such as altered protein conformation, however, this is purely speculative.

We observed maximal interaction between CAII and the cytosolic C terminus of NHE3 at pH 8 and above. Although there was some binding at the lower pH of our functional assays, the effect of an NHE3-CAII interaction would nonetheless be attenuated in our studies, underestimating its effect. Previous studies of sodium/proton exchangers found maximal transport activity when the cytosol was acidic. This makes intuitive sense for housekeeping transporters such as NHE1, as the role of this exchanger is to rid the cytosol of protons generated by metabolism. In this case, reduced activity at a physiological pH would prevent alkalinization of the cell. However, NHE3 does not appear to play a housekeeping role such as this; instead, it is implicit to the reabsorption of sodium from intestinal and renal epithelia and therefore plays a central role in volume regulation (28). Consequently, there may be a need to maintain NHE3 activity at physiological pH or even an alkaline pH. Perhaps the binding of CAII to the cytosolic terminus of NHE3 mediates this? NHE3 is activated by an acidic pH. However, functional studies have been performed predominantly in the absence of HCO_3^- and CO_2. Hence the activating effect of CAII on NHE3 activity would not have been recognized.

In summary, we show CO-IP of NHE3 with CAII, close association in renal epithelial cells, and direct interaction by GST-binding studies. This physical interaction between NHE3 and CAII contributes to increased NHE3 activity. However, a physical interaction is insufficient to increase NHE3 activity as CAII catalysis is also required. Thus NHE3 and CAII both physically and functionally interact, an association likely facilitating the vast amount of salt and water reabsorption from the proximal tubule and intestine.

Acknowledgments

GRANTS

This work was funded by grants from the Canadian Institute of Health Research (CIHR) to R. T. Alexander (MOP106464), E. Cordat (MOP106565), and J. R. Casey (MOP123452). D. Krishnan is supported by a graduate studentship from the Women and Children's Health Research Institute. A Clinician Scientist Award from CIHR and an Alberta Innovates Health Solutions Clinical Investigator Award support R. T. Alexander.

References

1. Al-Samir S, Papadopoulos S, Scheibe RJ, Meissner JD, Cartron JP, Sly WS, Alper SL, Gros G, Endeward V. Activity and distribution of intracellular carbonic anhydrase II and their effects on the transport activity of anion exchanger AE1/SLC4A1. J Physiol. 2013; 591:4963–4982. [PubMed: 23878365]
2. Alexander RT, Furuya W, Szászi K, Orlowski J, Grinstein S. Rho GTPases dictate the mobility of the Na/H exchanger NHE3 in epithelia: role in apical retention and targeting. Proc Natl Acad Sci USA. 2005; 102:12253–12258. [PubMed: 16103375]
3. Alexander RT, Malevanets A, Durkan AM, Kocinsky HS, Aronson PS, Orlowski J, Grinstein S. Membrane curvature alters the activation kinetics of the epithelial Na^+/H^+ exchanger, NHE3. J Biol Chem. 2007; 282:7376–7384. [PubMed: 17218318]
4. Almomani EY, King JC, Netsawang J, Yenchitsomanus PT, Malasit P, Limjindaporn T, Alexander RT, Cordat E. Adaptor protein 1 complexes regulate intracellular trafficking of the kidney anion exchanger 1 in epithelial cells. Am J Physiol Cell Physiol. 2012; 303:C554–C566. [PubMed: 22744004]
5. Alvarez BV, Vithana EN, Yang Z, Koh AH, Yeung K, Yong V, Shandro HJ, Chen Y, Kolatkar P, Palasingam P, Zhang K, Aung T, Casey JR. Identification and characterization of a novel mutation in the carbonic anhydrase IV gene that causes retinitis pigmentosa. Invest Ophthalmol Vis Sci. 2007; 48:3459–3468. [PubMed: 17652713]
6. Becker HM, Deitmer JW. Carbonic anhydrase II increases the activity of the human electrogenic Na^+/cotransporter. J Biol Chem. 2007; 282:13508–13521. [PubMed: 17353189]
7. Becker HM, Deitmer JW. Nonenzymatic proton handling by carbonic anhydrase II during H^+-lactate cotransport via monocarboxylate transporter 1. J Biol Chem. 2008; 283:21655–21667. [PubMed: 18539591]
8. Becker HM, Klier M, Schuler C, McKenna R, Deitmer JW. Intramolecular proton shuttle supports not only catalytic but also noncatalytic function of carbonic anhydrase II. Proc Natl Acad Sci USA. 2011; 108:3071–3076. [PubMed: 21282642]
9. Biemesderfer D, Rutherford PA, Nagy T, Pizzonia JH, Abu-Alfa AK, Aronson PS. Monoclonal antibodies for high-resolution localization of NHE3 in adult and neonatal rat kidney. Am J Physiol Renal Physiol. 1997; 273:F289–F299.
10. Bobulescu IA, Dubree M, Zhang J, McLeroy P, Moe OW. Effect of renal lipid accumulation on proximal tubule Na^+/H^+ exchange and ammonium secretion. Am J Physiol Renal Physiol. 2008; 294:F1315–F1322. [PubMed: 18417539]
11. Bondy C, Chin E, Smith BL, Preston GM, Agre P. Developmental gene expression and tissue distribution of the CHIP28 water-channel protein. Proc Natl Acad Sci USA. 1993; 90:4500–4504. [PubMed: 8506291]
12. Dirks JH, Cirksena WJ, Berliner RW. Micropuncture study of the effect of various diuretics on sodium reabsorption by the proximal tubules of the dog. J Clin Invest. 1966; 45:1875–1885. [PubMed: 5926633]
13. Donowitz M, Ming Tse C, Fuster D. SLC9/NHE gene family, a plasma membrane and organellar family of Na^+/H^+ exchangers. Mol Aspects Med. 2013; 34:236–251. [PubMed: 23506868]
14. Fuster DG, Alexander RT. Traditional and emerging roles for the SLC9 Na^+/H^+ exchangers. Pflügers Arch. 2014; 466:61–76. [PubMed: 24337822]
15. Gawenis LR, Stien X, Shull GE, Schultheis PJ, Woo AL, Walker NM, Clarke LL. Intestinal NaCl transport in NHE2 and NHE3 knockout mice. Am J Physiol Gastrointest Liver Physiol. 2002; 282:G776–G784. [PubMed: 11960774]
16. Li X, Alvarez B, Casey JR, Reithmeier RAF, Fliegel L. Carbonic anhydrase II binds to and enhances activity of the Na^+/H^+ exchanger. J Biol Chem. 2002; 277:36085–36091. [PubMed: 12138085]
17. Li X, Liu Y, Alvarez BV, Casey JR, Fliegel L. A novel carbonic anhydrase II binding site regulates NHE1 activity. Biochemistry. 2006; 45:2414–2424. [PubMed: 16475831]

18. Okamoto K, Hanazaki K, Akimori T, Okabayashi T, Okada T, Kobayashi M, Ogata T. Immunohistochemical and electron microscopic characterization of brush cells of the rat cecum. Med Mol Morphol. 2008; 41:145–150. [PubMed: 18807140]
19. Orlowski J, Kandasamy RA, Shull GE. Molecular cloning of putative members of the Na/H exchanger gene family. cDNA cloning, deduced amino acid sequence, and mRNA tissue expression of the rat Na/H exchanger NHE-1 and two structurally related proteins. J Biol Chem. 1992; 267:9331–9339. [PubMed: 1577762]
20. Pan W, Borovac J, Spicer Z, Hoenderop JG, Bindels RJ, Shull GE, Doschak MR, Cordat E, Alexander RT. The epithelial sodium/proton exchanger, NHE3, is necessary for renal and intestinal calcium (re)absorption. Am J Physiol Renal Physiol. 2012; 302:F943–F956. [PubMed: 21937605]
21. Parkkila S. Distribution of the carbonic anhydrase isoenzyme I, II, and VI in the human alimentary tract. Gut. 1994; 35:646–650. [PubMed: 8200558]
22. Piermarini PM, Kim EY, Boron WF. Evidence against a direct interaction between intracellular carbonic anhydrase II and pure C-terminal domains of SLC4 bicarbonate transporters. J Biol Chem. 2007; 282:1409–1421. [PubMed: 17090540]
23. Prasad GV, Coury LA, Finn F, Zeidel ML. Reconstituted aquaporin 1 water channels transport CO_2 across membranes. J Biol Chem. 1998; 273:33123–33126. [PubMed: 9837877]
24. Pushkin A, Abuladze N, Gross E, Newman D, Tatishchev S, Lee I, Fedotoff O, Bondar G, Azimov R, Ngyuen M, Kurtz I. Molecular mechanism of kNBC1, carbonic anhydrase II interaction in proximal tubule cells. J Physiol. 2004; 559:55–65. [PubMed: 15218065]
25. Rievaj J, Pan W, Cordat E, Alexander RT. The Na^+/H^+ exchanger isoform 3 is required for active paracellular and transcellular Ca^{2+} transport across murine cecum. Am J Physiol Gastrointest Liver Physiol. 2013; 305:G303–G313. [PubMed: 23764894]
26. Rubio CR, de Mello GB, Mangili OC, Malnic G. H^+ ion secretion in proximal tubule of low-CO2/HCO3- perfused isolated rat kidney. Pflügers Arch. 1982; 393:63–70. [PubMed: 6806771]
27. Schnermann J, Chou CL, Ma T, Traynor T, Knepper MA, Verkman AS. Defective proximal tubular fluid reabsorption in transgenic aqua-porin-1 null mice. Proc Natl Acad Sci USA. 1998; 95:9660–9664. [PubMed: 9689137]
28. Schultheis PJ, Clarke LL, Meneton P, Miller ML, Soleimani M, Gawenis LR, Riddle TM, Duffy JJ, Doetschman T, Wang T, Giebisch G, Aronson PS, Lorenz JN, Shull GE. Renal and intestinal absorptive defects in mice lacking the NHE3 Na^+/H^+ exchanger. Nat Genet. 1998; 19:282–285. [PubMed: 9662405]
29. Sjöblom M, Singh AK, Zheng W, Wang J, Tuo Bg, Krabbenhöft A, Riederer B, Gros G, Seidler U. Duodenal acidity sensing, but not epithelial HCO_3, supply is critically dependent on carbonic anhydrase II expression. Proc Natl Acad Sci USA. 2009; 106:13094–13099. [PubMed: 19622732]
30. Soderberg O, Gullberg M, Jarvius M, Ridderstrale K, Leuchowius KJ, Jarvius J, Wester K, Hydbring P, Bahram F, Larsson LG, Landegren U. Direct observation of individual endogenous protein complexes in situ by proximity ligation. Nat Methods. 2006; 3:995–1000. [PubMed: 17072308]
31. Srere PA, Sumegi B, Sherry AD. Organizational aspects of the citric acid cycle. Biochem Soc Symp. 1987; 54:173–178. [PubMed: 3332994]
32. Sterling D, Alvarez BV, Casey JR. The extracellular component of a transport metabolon: extracellular loop 4 of the human AE1 Cl-/HCO3- exchanger binds carbonic anhydrase IV. J Biol Chem. 2002; 277:25239–25246. [PubMed: 11994299]
33. Sterling D, Reithmeier RAF, Casey JR. A transport metabolon: functional interaction of carbonic anhydrase II and chloride/bicarbonate exchangers. J Biol Chem. 2001; 276:47886–47894. [PubMed: 11606574]
34. Thomas JA, Buchsbaum RN, Zimniak A, Racker E. Intracellular pH measurements in Ehrlich ascites tumor cells utilizing spectroscopic probes generated in situ. Biochemistry. 1979; 18:2210–2218. [PubMed: 36128]
35. Tse CM, Levine SA, Yun CH, Brant SR, Pouyssegur J, Montrose MH, Donowitz M. Functional characteristics of a cloned epithelial Na^+/H^+ exchanger (NHE3): resistance to amiloride and inhibition by protein kinase C. Proc Natl Acad Sci USA. 1993; 90:9110–9114. [PubMed: 8415663]

36. Vilas G, Krishnan D, Loganathan SK, Malhotra D, Liu L, Beggs MR, Gena P, Calamita G, Jung M, Zimmermann R, Tamma G, Casey JR, Alexander RT. Increased water flux induced by an aquaporin-1/carbonic anhydrase II interaction. Mol Biol Cell. 2015; 26:1106–1118. [PubMed: 25609088]
37. Vince JW, Carlsson U, Reithmeier RAF. Localization of the Cl-/HCO3- anion exchanger binding site to the amino-terminal region of carbonic anhydrase II. Biochemistry. 2000; 39:13344–13349. [PubMed: 11063570]
38. Vince JW, Reithmeier RA. Carbonic anhydrase II binds to the carboxyl terminus of human band 3, the erythrocyte Cl-/HCO3- exchanger. J Biol Chem. 1998; 273:28430–28437. [PubMed: 9774471]
39. Vince JW, Reithmeier RAF. Identification of the carbonic anhydrase II binding site in the Cl-/HCO3- anion exchanger AE1. Biochemistry. 2000; 39:5527–5533. [PubMed: 10820026]
40. Waheed A, Zhu XL, Sly WS, Wetzel P, Gros G. Rat skeletal muscle membrane associated carbonic anhydrase is 39-kDa, glycosylated, GPI-anchored CA IV. Arch Biochem Biophys. 1992; 294:550–556. [PubMed: 1533109]
41. Zhang J, Tackaberry T, Ritzel MW, Raborn T, Barron G, Baldwin SA, Young JD, Cass CE. Cysteine-accessibility analysis of transmembrane domains 11–13 of human concentrative nucleoside transporter 3. Biochem J. 2006; 394:389–398. [PubMed: 16271041]

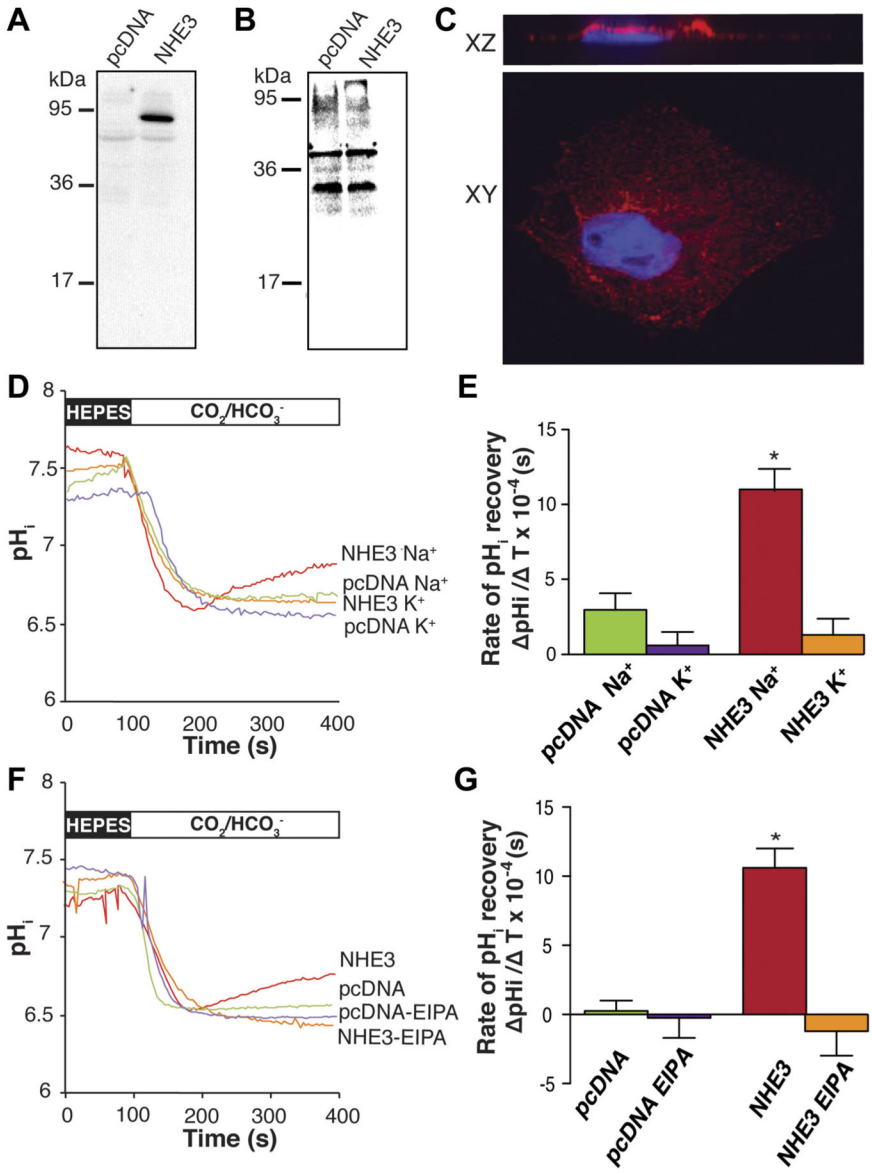

Fig. 1.

Opossum kidney (OK) cells overexpressing sodium/proton exchanger isoform 3 (NHE3) demonstrate increased sodium-dependent recovery of pH. NHE3 with 3 exofacial hemagglutinin (HA) tags ($NHE3_{38HA3}$) was stably expressed in OK cells. Lysates from cells stably expressing $NHE3_{38HA3}$ or pcDNA were immunoblotted with anti-HA antibody (*A*) or anti-carbonic an-hydrase II (CAII) antibody (*B*). *C*: *XY* and *XZ* confocal image of a polarized OK cell immunostained with anti-HA (red) and 4,6-diamidino-2-phenylindole (DAPI; blue). *D*–*G*: assessment of NHE3 activity. Cells loaded with the pH-sensitive fluorescent probe BCECF-AM were acidified by switching them from HEPES-buffered medium to one containing CO_2/HCO_3^- (either as a Na^+ or K^+ salt; the switch is represented as a change from a black to a white bar). *D*: representative traces of the change in intracellular pH (pH_i) of cells either stably expressing $NHE3_{38HA3}$ or pcDNA (-ve control) over time in the presence of extracellular sodium (Na^+) or absence of extracellular sodium

(K^+). Note: results were similar when choline- Cl^-/HCO_3^- was used. *F*: representative traces of the change in pH_i of cells either stably expressing $NHE3_{38HA3}$ or pcDNA (-ve control) in the presence and absence of 100 μM EIPA. *E* and *G*: quantification of initial change (Δ) in pH (over the first 30 s) for each condition displayed in *D* or *F*. $*P < 0.05$; $n =$ >6/condition.

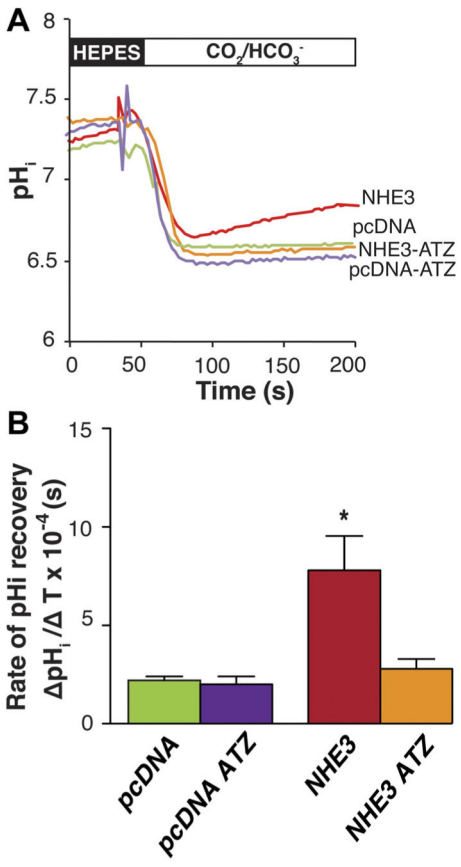

Fig. 2.

The carbonic anhydrase inhibitor acetazolamide (ATZ) inhibits NHE3. *A*: representative traces of the initial change in pH_i after intracellular acidification induced by switching from a HEPES-buffered solution to one containing HCO_3^- and bubbled with 5% CO_2; the timing of the switch is indicated by the change from a black bar to a white bar over the trace. Traces are from OK cells stably expressing either $NHE3_{38HA3}$ or pcDNA in the presence and absence of 100 μM ATZ. *B*: quantification of initial NHE3 activity (over the first 30 s) for each condition displayed in *A*. **P* < 0.01; *n* = > 6/condition.

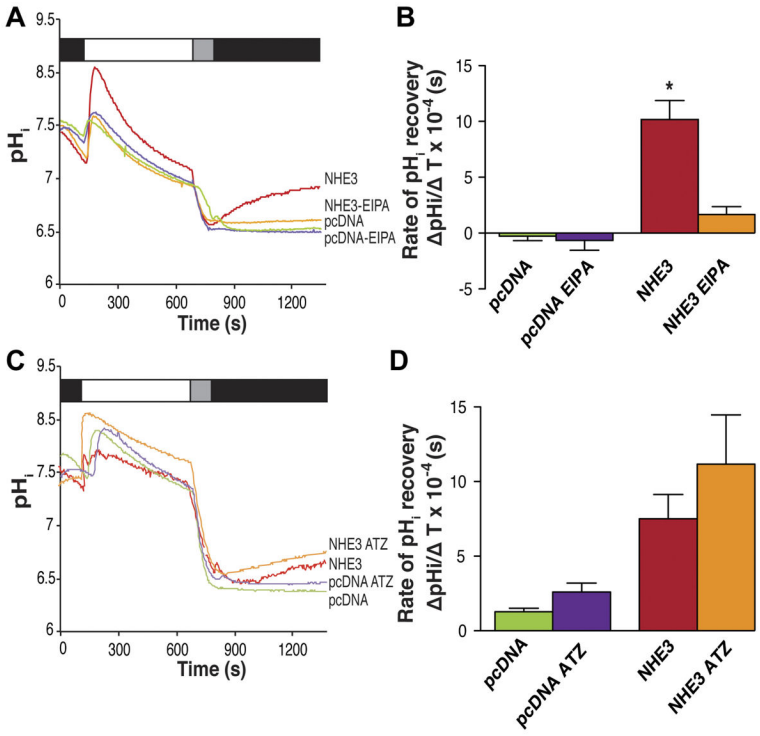

Fig. 3.

ATZ does not inhibit NHE3 activity in the absence of CO_2. NHE3 activity was assessed in the absence of CO_2 and HCO_3^- by prepulsing the cells with NH_4Cl. *A*: representative traces of the change in pH_i of OK cells expressing either $NHE3_{38HA3}$ or pcDNA (negative control) in the presence and absence of 100 μM EIPA. Above the traces is a bar representing the different perfusing solutions: black, Na^+ containing; white, NH_4Cl prepulse; grey, no Na^+ containing buffer. *B*: quantification of initial NHE3 activity (over the first 30 s) for each condition displayed in *A*. $*P < 0.01$. *C*: representative traces of the change in pH_i of cells stably expressing either $NHE3_{38HA3}$ or pcDNA (-ve control) in the presence and absence of 100 μM ATZ. The bar above the traces is as described for *A*. *D*: quantification of initial NHE3 activity (over the first 100s) for each condition displayed in *C*; n = >6/condition.

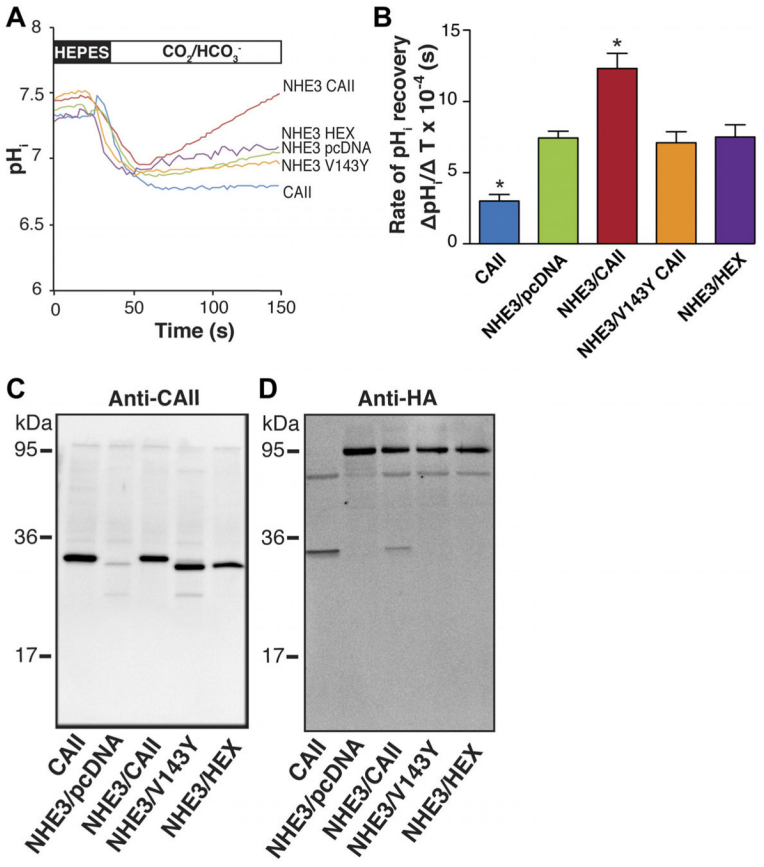

Fig. 4.

CAII activity and binding are required to enhance NHE3 activity. *A*: representative images of the change in pH_i of OK cells transfected with either NHE3 and CAII, NHE3 and CAII-V143Y (functionally inactive mutant), CAII alone, NHE3 and CAII-HEX (functionally active but can't bind transporters), or pcDNA and NHE3 after acidification induced by switching from a HEPES-buffered solution to one containing HCO_3^-, and bubbled with 5% CO_2. The change in perfusion buffers is represented by a change from a black to a white bar above the traces. *B*: quantification of initial NHE3 activity (over the first 30 s) for each condition displayed in *A*. $*P < 0.001$ relative to NHE3- and pcDNA-transfected cells. *C* and *D*: immunoblots of cell lysate from experiments in *A* and *B* to determine CAII (*C*) or HA (NHE3) expression (*D*).

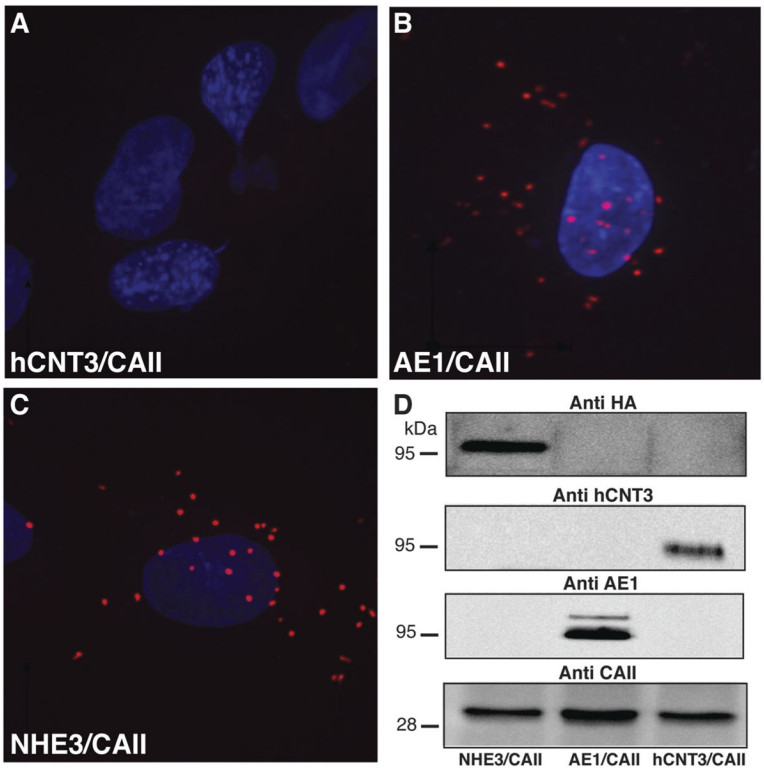

Fig. 5.

CAII associates closely with NHE3. Representative images are shown from a proximity ligation assay performed on OK cells transfected with CAII and either hCNT3 (negative control; *A*), AE1 (positive control; *B*), or NHE3 (*C*). Note: in all representative images (*A*–*C*), the nuclei was stained with DAPI (blue). *D*: immunoblots probed for hCNT3, AE1, HA (for NHE3), and CAII on lysate from cells expressing NHE3 and CAII, AE1 and CAII, or hCNT3 and CAII.

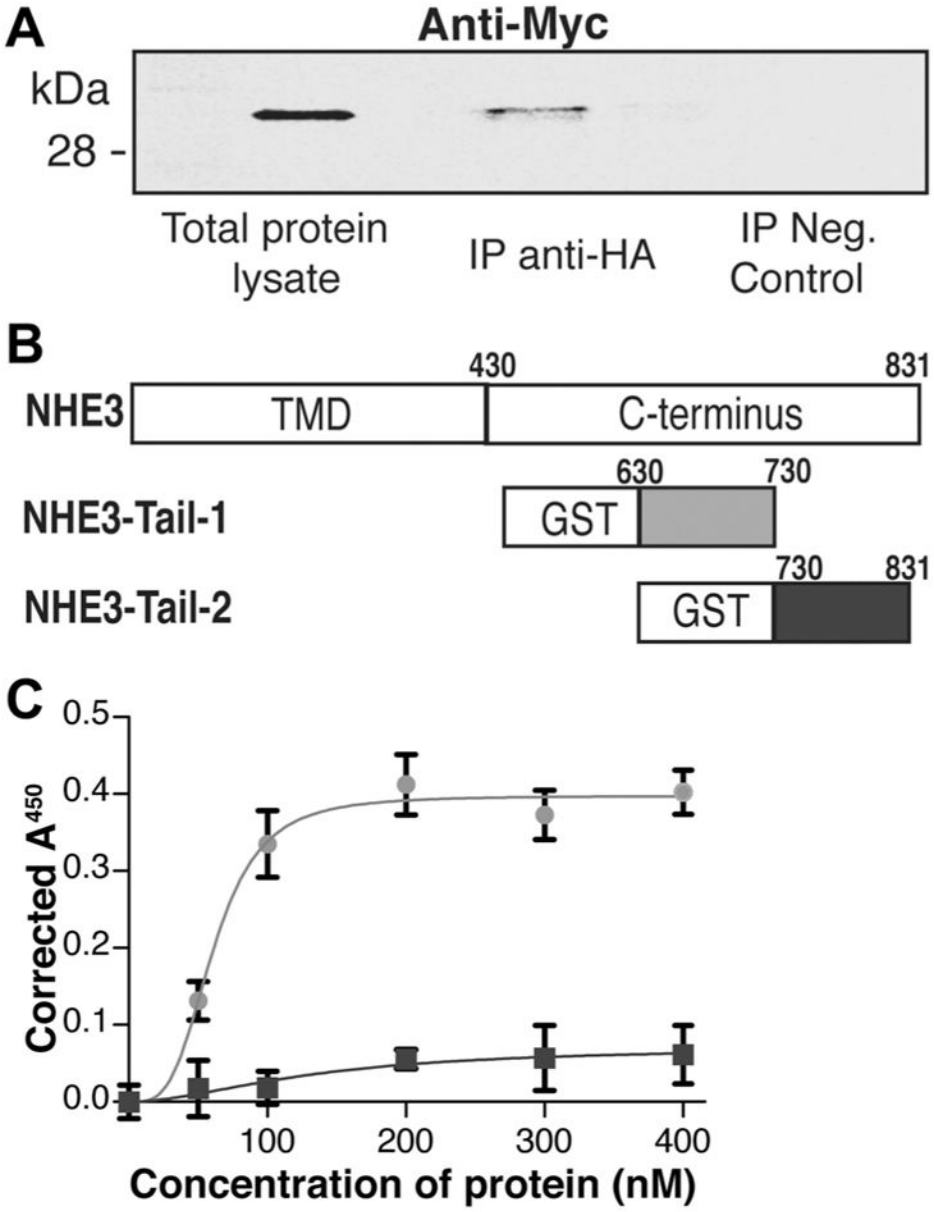

Fig. 6.

CAII binds the C terminus of NHE3. *A*: NHE3-CAII coimmunoprecipitation (IP). OK cells cotransfected with $NHE3_{38HA3}$ and CAII-myc were lysed and immunoprecipitated with either anti-HA (to pull down NHE3) or in the presence of rabbit IgG (negative control) and then immunoblotted for anti-myc (CAII). A sample of total protein lysate was included. Note: a blank lane was left between samples on the gel. *B*: schematic representation of the glutathione-*S*-transferase (GST)-fusion constructs generated from the cytosolic carboxy terminus of NHE3. Note: NHE3-Tail-1 contains a potential CAII binding site homolgous to NHE1 (^{710}IKEKDLELSDTEE^{722}). *C*: CAII was fixed to a 96-well plate, which was subsequently overlaid with the concentration of the GST-fusion protein listed on the *x*-axis. After washing, the samples were incubated with an anti-GST antibody and then the

appropriate secondary antibody. The net relative amount of GST-fusion protein binding was assessed by a colorimetric reaction measured at A_{450}, which is subtracted from the background obtained with only GST protein.

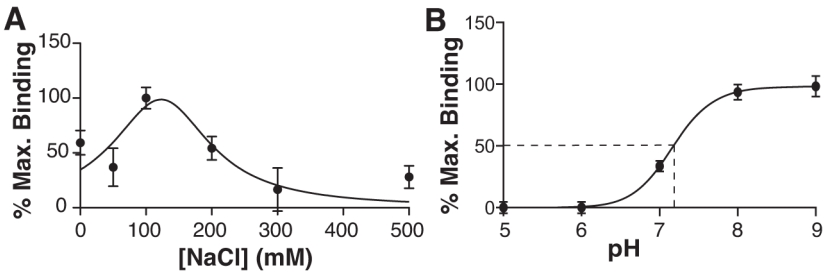

Fig. 7.

CAII binding to the C terminus of NHE3 is NaCl concentration and pH sensitive. *A*: a microtitre plate binding assay was used to probe the nature of the physical interaction between NHE3 and CAII as per Fig. 6. However, the antibody buffer used to apply the fusion proteins contained varying concentrations of NaCl, from 100–500 mM or a range of pH (5–9). Note: results are corrected for the background obtained with only GST protein as above.